Thermochemical purification of talc with ammonium sulphate as chemical additive

Barbara A. Castleman[a], Elizabet M. van der Merwe[a] and Frédéric J. Doucet[b]*

[a] Department of Chemistry, University of Pretoria, Lynnwood Road, Pretoria 0002, South Africa

[b] Council for Geoscience, Private Bag X112, Pretoria 0001, South Africa

*Corresponding author. Tel: +27 (0) 12 4205379. E-mail address: liezel.vandermerwe@up.ac.za

Highlights

- Talc reactivity during thermochemical treatment with ammonium sulphate was studied
- Talc was unaltered during the studied process
- This process represents a promising technology for the purification of talc

Competing interest statement

The authors declare that they have no known competing financial interests or personal relationships that could have appeared to influence the work reported in this paper.

Abstract

This study reports on the thermochemical reactivity of talc with ammonium sulphate, a low-cost, recyclable chemical additive commonly used in the thermochemical extraction of strategic metals from low-grade ores and industrial and mine residues. The talc sample used in this study contained 70% talc, 15% lizardite and 10% kaolinite, following the removal of carbonate minerals by HCl leaching as a pre-concentration step. The solid product obtained by thermochemical treatment followed by aqueous leaching contained high-grade purified talc (>98%) as the principal mineral phase. It was depleted from lizardite and kaolinite, which had reacted with ammonium sulphate to form water-soluble hydrated ammonium metal sulphates. A comparative analysis of the TGA profiles of the concentrated parent sample, the solid product and the solid residue highlighted an identical mass loss between 850°C and 1000°C, which is the temperature range at which the dehydroxylation of talc occurs. This indicated minimal, if any, structural denaturation of the talc phase following thermochemical treatment with ammonium sulphate under the experimental condition studied. This process may therefore represent a promising technology for the purification of talc under the right market conditions, provided the mineral co-exists with phases featuring a high degree of reactivity with ammonium sulphate under thermal conditions.

Keywords:

Talc; purification; ammonium sulphate; thermochemical treatment; thermogravimetric analysis

1. Introduction

Talc is a naturally-occurring hydrated magnesium-rich sheet phyllosilicate with the ideal chemical formula $Mg_3Si_4O_{10}(OH)_2$ (Martin et al., 2019). Although it is the least complex phyllosilicate, natural talc varies greatly in colour, grain size, crystallinity, lamellar-character, softness, and chemical composition, depending on its geological origin (Soriano et al., 2002). Talc deposits can derive from a variety of parent rocks, which include magnesium carbonates, serpentines, aluminosilicate rocks, or magnesium sedimentary deposits (Zussman et al., 2013). As a result, talc ore is found to co-exist with a number of accessory (gangue) minerals, including chlorite, lizardite and carbonates (magnesite, calcite, dolomite). These gangues represent mineral hydrophilic impurities (Castillo et al., 2014), which must be removed before talc can meet the requirements of specific industrial applications such as paints, plastics, medicine or cosmetics.

The purification of low-grade talc ores represents an area of great interest, owing to the limitations, economics and environmental impacts of current technologies, and the wide array of possible accessory minerals associated with talc and their distinct intrinsic reactivities. Examples of such technologies include flotation, wet attrition, magnetic separation, and acid leaching (Table 1; Piga and Marruzzo, 1992; Ahmed et al., 2007; Hojamberdiev et al., 2010; Orosco et al, 2011; Dumas et al., 2015; Barani and Aghazadeh, 2018; Katircioglu-Bayel, D., 2020).

Table 1 Comparison of advantages and disadvantages of talc purification methods

Purification Method	Advantages	Disadvantages
Flotation (Ahmed et al., 2007)	• No chemical changes occur • Carbonate minerals remain intact	• Accessory chemicals required • High cost • Specialised equipment required • Multistep processes, often followed by acid leaching
Wet attrition (Katircioglu-Bayel, D., 2020.)	• Likely to produce finer ground products	
Magnetic Separation (Piga and Marruzzo, 1992; Hojamberdiev et al., 2010)	• Reduces the iron content	
Chlorination (Orosco et al, 2011)	• Removes Fe_2O_3 efficiently • Improves colour	• Corrosive atmosphere • Specialised equipment required
Acid Leaching (Ahmed et al., 2007; Orosco et al, 2011; Barani and Aghazadeh, 2018)	• Removes carbonate impurities efficiently, and Fe_2O_3 to some degree • No specialised equipment required	• Carbonate minerals are lost

Thermochemical treatment using ammonium sulphate ($(NH_4)_2SO_4$) is an actively researched technology for the extraction of strategic metals from several mineral-bearing materials. Examples include coal fly ash (Wu et al., 2014; Doucet et al., 2016), laterite nickel ore (Li et al., 2018), PGM tailings (Mohamed et al., 2016, 2019), and bauxite residue (Borra et al., 2016). This process can also be successfully applied for the extraction of magnesium from serpentinite rocks in the context of CO_2 mineral sequestration (Nduagu et al., 2012). However, different serpentine minerals display varying degrees of reactivity with $(NH_4)_2SO_4$, which is mostly guided by their mineralogical structure, their parent rock, and any possible transformation the rock may have undergone through metamorphosis

or other type of alteration (Lavikko and Eklund, 2016a). For instance, lizardite appears to pair the favourable features more often than antigorite (Sjöblom and Eklund, 2014; Lavikko and Eklund, 2016b), which generally makes it a more suitable parent material for mineral carbonation.

The co-existence of lizardite as accessory mineral in South African talc ore, and the fact that talc is characterised by little chemical reactivity, have raised the question as to whether talc ore could be purified via thermal treatment with $(NH_4)_2SO_4$. The primary objective of this paper is therefore to report on the suitability of thermochemical processing with $(NH_4)_2SO_4$ as a promising new technology for the purification of talc. An outline of the multi-stage purification process is illustrated in Figure 1.

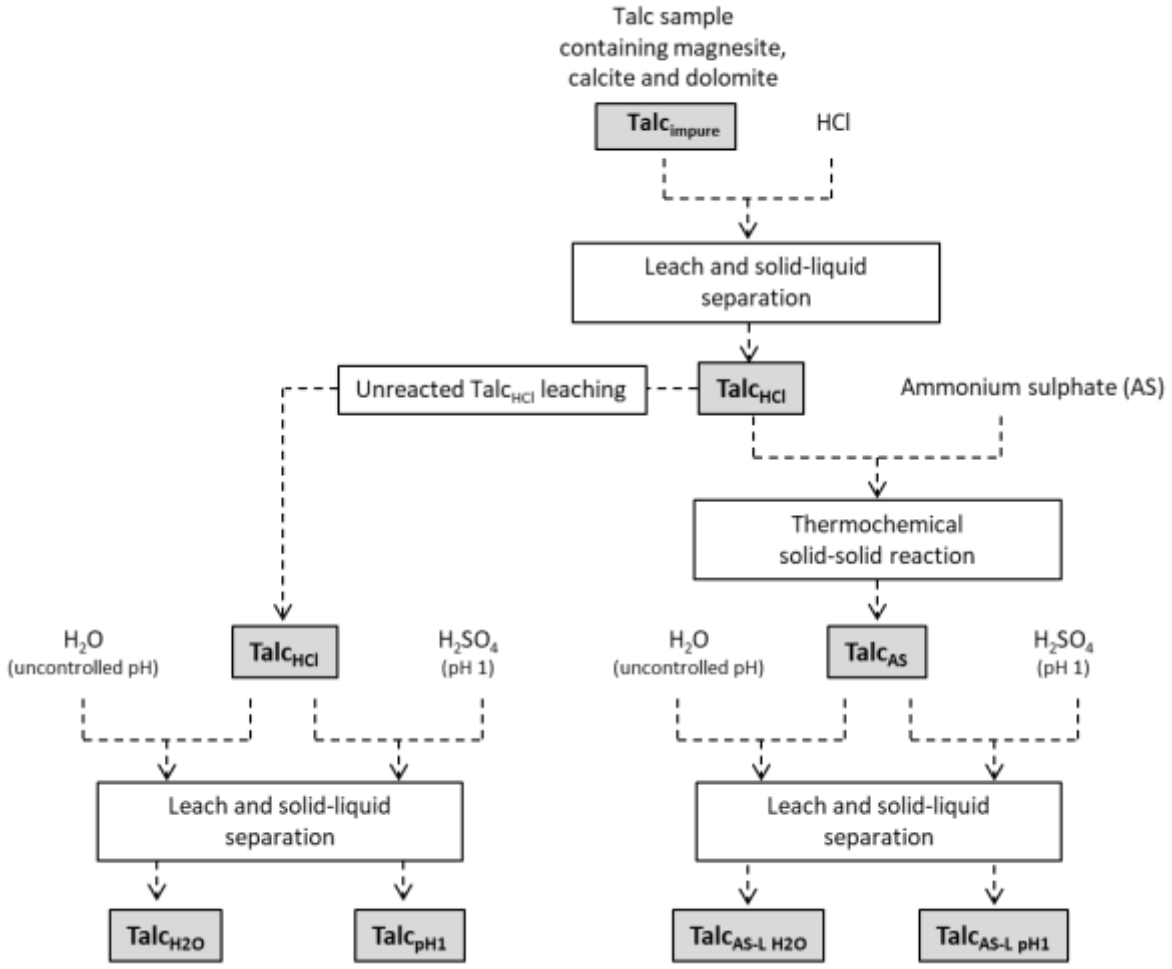

Figure 1 Process flow diagram for direct leaching (Control) and thermochemical treatment followed by leaching (Treatment) of talc-bearing samples. Aqueous phases are not included.

2. Materials and Methods

2.1. Material tested, chemical reagents and pre-treatment

A talc sample was obtained from the Scotia Talc Mine, which is located near Barberton in the province of Mpumalanga, South Africa. XRD analysis revealed the presence of carbonate minerals (magnesite, calcite and dolomite). The sample (hereafter denoted $Talc_{impure}$) was therefore pre-treated with 10% m/m hydrochloric acid (HCl) to induce their dissolution (Castillo et al, 2011) and concentrate the talc phase. This pre-concentration step generated the talc-rich solid residue (hereafter denoted $Talc_{HCl}$), which was used in all further experiments. The use of a FRITSCH analysette SPARTAN sieve shaker revealed that 83% m/m of $Talc_{HCl}$ was < 125µm.

Ammonium sulphate ($(NH_4)_2SO_4$; hereafter denoted AS), deionised water and acids used were all AR grade and were sourced from Merck Chemicals (Pty) Ltd.

2.2. Thermochemical treatment and leaching of talc

A flow diagram illustrating the studied process is given in Figure 1.$Talc_{HCl}$ was thoroughly mixed with AS, at a 2:3 m/m ratio. The resulting mixture was thermally treated in a muffle furnace at 450 ^{o}C for 60 minutes. The quantity of AS used represented a stoichiometric excess in relation to the total content of magnesium in $Talc_{HCl}$. The temperature was selected to ensure that AS loss was minimised during thermochemical treatment, allowing AS to be recycled at a subsequent stage. The selected duration of the thermochemical treatment ensured good flowability of the powdered reaction product after thermochemical treatment (Mohamed et al., 2019).

At completion of the thermochemical treatment, the product of the reaction ($Talc_{AS}$) was leached in deionised water (uncontrolled pH condition) or sulphuric acid (H_2SO_4; pH = 1.0) using a ratio of 1:100

(m/v) at 50^{o}C. Samples were stirred using a magnetic stirrer at a rate of 750 rpm. The pH, conductivity and temperature of the suspensions were monitored throughout the leaching process. The leaching process was ended when there was no further change in the conductivity reading. The $Talc_{HCl}$ sample (i.e. not thermochemically treated) was also leached, under both uncontrolled and controlled pH conditions, and used as controls. At completion of the leaching process, samples were filtered through a Sartorius polycarbonate Track-Etch membrane. The leach residues ($Talc_{AS\text{-}L\ H2O}$, $Talc_{AS\text{-}L\ pH1}$, $Talc_{L\ H2O}$ and $Talc_{L\ pH1}$) were washed with distilled water, dried at 100^{o}C overnight and characterised using a set of complementary techniques.

2.3. Structural and textural characterisation of parent talc, $Talc_{HCl}$ and residues

Chemical compositions of the talc samples were obtained using XRF (Thermo Fisher Perform'X Sequential XRF with OXSAS software). The loss on ignition (LOI) was determined by roasting the sample at 1000 °C for at least 3 h until a constant weight was obtained. Mineralogical compositions of the talc samples were obtained using XRD (PANalytical X'Pert Pro powder diffractometer). Mineral phase concentrations were determined by Rietveld quantitative analysis with Highscore software with accuracy in the region of ±1%.

TGA analyses were performed on a TA Instruments SDT Q600 Thermogravimetric Analyzer & Differential Scanning Calorimeter (DSC). Approximately 18 mg of sample was placed in an alumina pan and heated from 25 to 1100 ^{o}C at a heating rate of 10 ^{o}C/min. Each test was conducted using a flow rate of 100 mL/min of nitrogen (N_2).

A Bruker Platinum ATR (attenuated total reflectance) instrument, with a diamond crystal, was used to record FTIR spectra in the 4000 – 500 cm^{-1} range. All spectra were collected with 64 scans per background and per sample, and analysed using the OPUS software. These were compared to spectra from pure laboratory chemicals as well as spectra stored in the RRuff Database.

A Zeiss Ultra PLUS FEG SEM instrument, operating at an accelerated voltage of 1 kV, was used to obtain information on the morphology and surface features of the samples. Samples were mounted on a metal substrate by means of a double-sided carbon tape and subsequently sputter-coated with a thin, conductive layer of carbon using an Emitech K550X coater (Ashford, England).

3. Results and discussion

3.1. Characterisation of parent talc and $Talc_{HCl}$

The parent talc sample obtained from the Scotia Talc Mine contained 33.5% m/m talc and a substantial amount of carbonate minerals (47.0 % magnesite, 3.3% dolomite and 1.2% calcite), as well as 8.3% lizardite, 3.9% kaolinite, and minor quantities of quartz and magnetite ($Talc_{impure}$; Figure 2). These impurities are commonly found in industrial talc, although their combination and concentrations depend on the origin of the sample (Alonso, 1991).

The talc content of $Talc_{impure}$ was too low to ascertain its reactivity with AS during thermochemical treatment. The sample was therefore pre-treated with 10% m/m HCl to remove the carbonate minerals and concentrate the talc phase. The talc concentrate ($Talc_{HCl}$) was mostly composed of 58.6% SiO_2, 30.2% MgO and 1.8% Fe_2O_3, and had a loss on ignition (LOI) of 8.7%. Its mineralogy (Table 2; Figure 2) consisted of talc ($Mg_3Si_4O_{10}(OH)_2$; ~68%), with smaller quantities of lizardite ($Mg_3Si_2O_5(OH)_4$; ~17%) and kaolinite ($A\ell_2Si_2O_5(OH)_4$; ~11%). This was confirmed by FTIR (Figure 3), which exhibited well-defined bands, specifically between 950 and 1050 cm^{-1}, where bending and stretching modes of the SiO_4^{2-} tetrahedron occurs (Hofmeister and Bowey, 2006), and which were consistent with these mineral phases. Thermogravimetric analysis of $Talc_{HCl}$ (Figure 4) indicated a total mass loss of 8.1% between ambient temperature and 1000°C, which confirmed the LOI value of 8.7%. It also showed a mass loss of 3.3% between 792 and 984^{o}C, which was attributed to the dehydroxylation and structural decomposition of talc into enstatite ($MgSiO_3$) and cristobalite (SiO_2), as shown by Equation 1 (Nakahira and Kato, 1963; de Souza Santos and Yada, 1988; Foldvari, 2011). The theoretical mass loss for the

dehydroxylation of talc according to Equation 1 is 4.8%. The mass loss associated to dehydroxylation of talc in $Talc_{HCl}$ (3.3%) therefore corresponds to a talc content of 68.8%.

$$Mg_3Si_4O_{10}(OH)_2\ (s) \rightarrow 3\ MgSiO_3\ (s) + SiO_2\ (s) + H_2O\ (g) \qquad \text{(Eq. 1)}$$

A combined mass loss of 3.8% was also observed between 550 – 650℃ and 600 - 780℃. These two regions correspond to the dehydroxylation of kaolinite (500 – 590℃) and lizardite (600 - 700°C) (Bayer et al, 1982; Földvári, 2011), which indicated a total content of 29.4% for these two mineral phases. The mineralogical compositions derived from TGA and XRD were therefore similar.

Table 2 Mineralogical compositions (wt.%) of concentrated parent sample ($Talc_{HCl}$), leach residue generated from the thermochemical treatment of $Talc_{HCl}$ with AS followed by leaching in H_2SO_4 at pH 1 ($Talc_{AS\text{-}L\ pH\ 1}$), and the 'control' leach residues following leaching of $Talc_{HCl}$ in either water ($Talc_{H2O}$) or H_2SO_4 at pH 1 ($Talc_{pH1}$).

Mineral	**Chemical Composition**	**$Talc_{HCl}$**	**$Talc_{AS\text{-}L\ pH\ 1}$**	**$Talc_{pH1}$**	**$Talc_{H2O}$**
Kaolinite	$Al_2Si_2O_5(OH)_4$	11.0	-	2.3	7.6
Lizardite	$Mg_3Si_2O_5(OH)_4$	17.2	1.2	17.0	21.6
Magnetite	Fe_3O_4	1.8	-	-	1.1
Quartz	SiO_2	2.9	-	0.5	2.1
Talc	$Mg_3Si_4O_{10}(OH)_2$	67.8	98.8	80.2	67.7

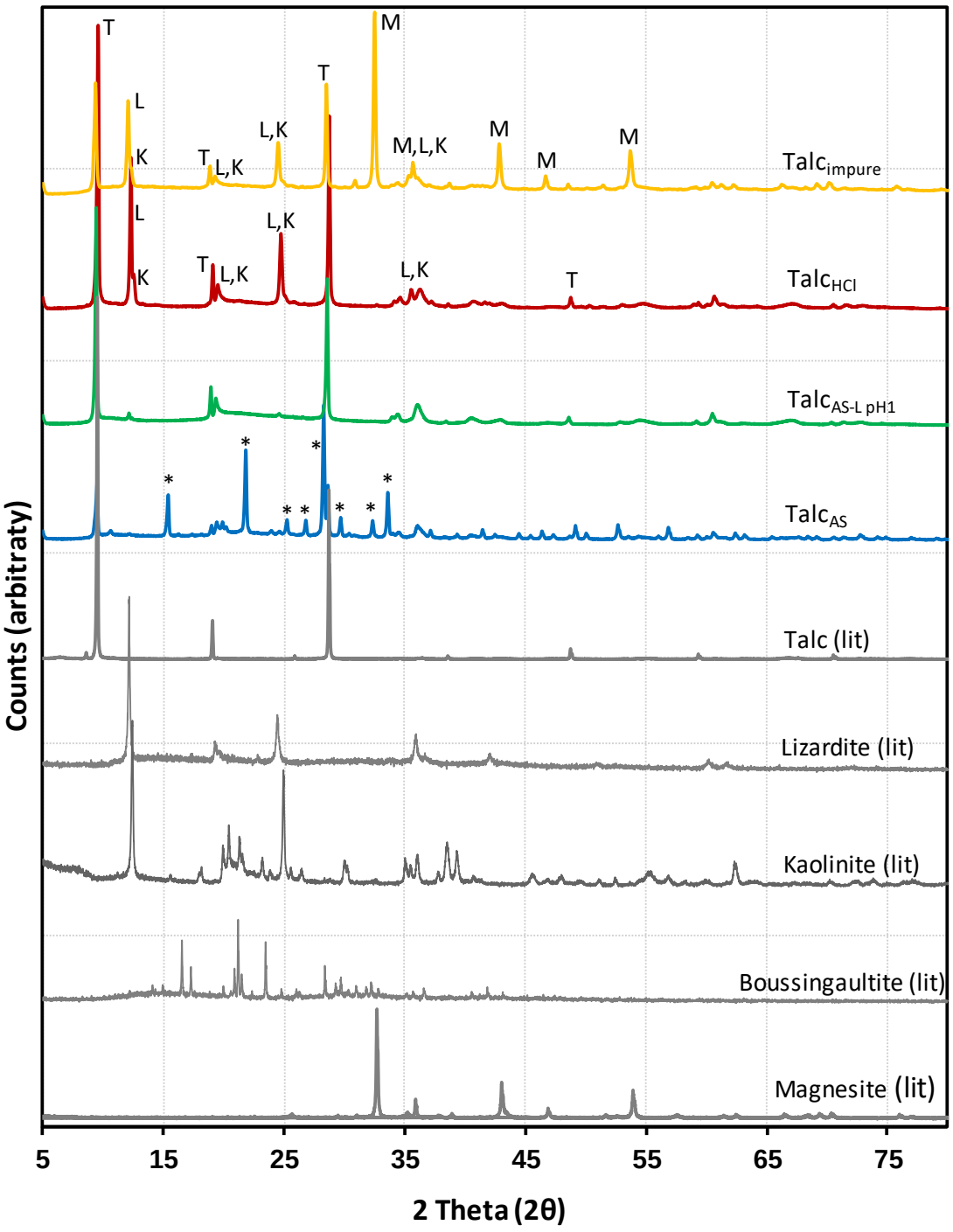

Figure 2 XRD patterns of Talc$_{impure}$ (yellow), Talc$_{HCl}$ (red), Talc$_{AS}$ (blue) and Talc$_{AS\text{-}L\ pH1}$ (green). Theoretical patterns of individual phases are also included (grey). T: talc, M: magnesite, L: lizardite, K: kaolinite. Peaks attributed to formation of sulphate species during thermochemical reaction are indicated with asterisks (*).

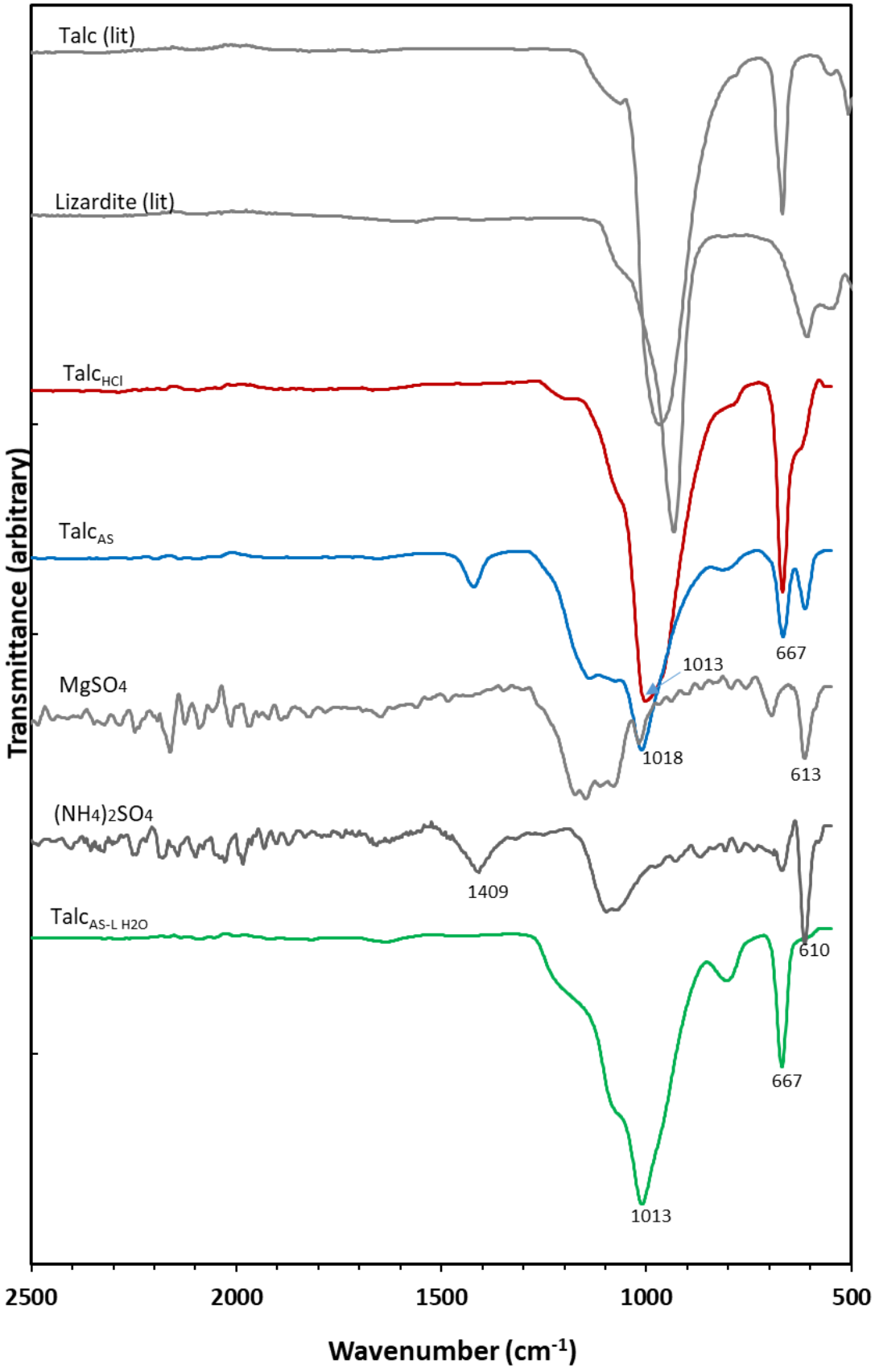

Figure 3 FTIR spectra for Talc$_{HCl}$ (red), Talc$_{AS}$ (blue), Talc$_{AS-L}$ (green) and pure salts (grey).

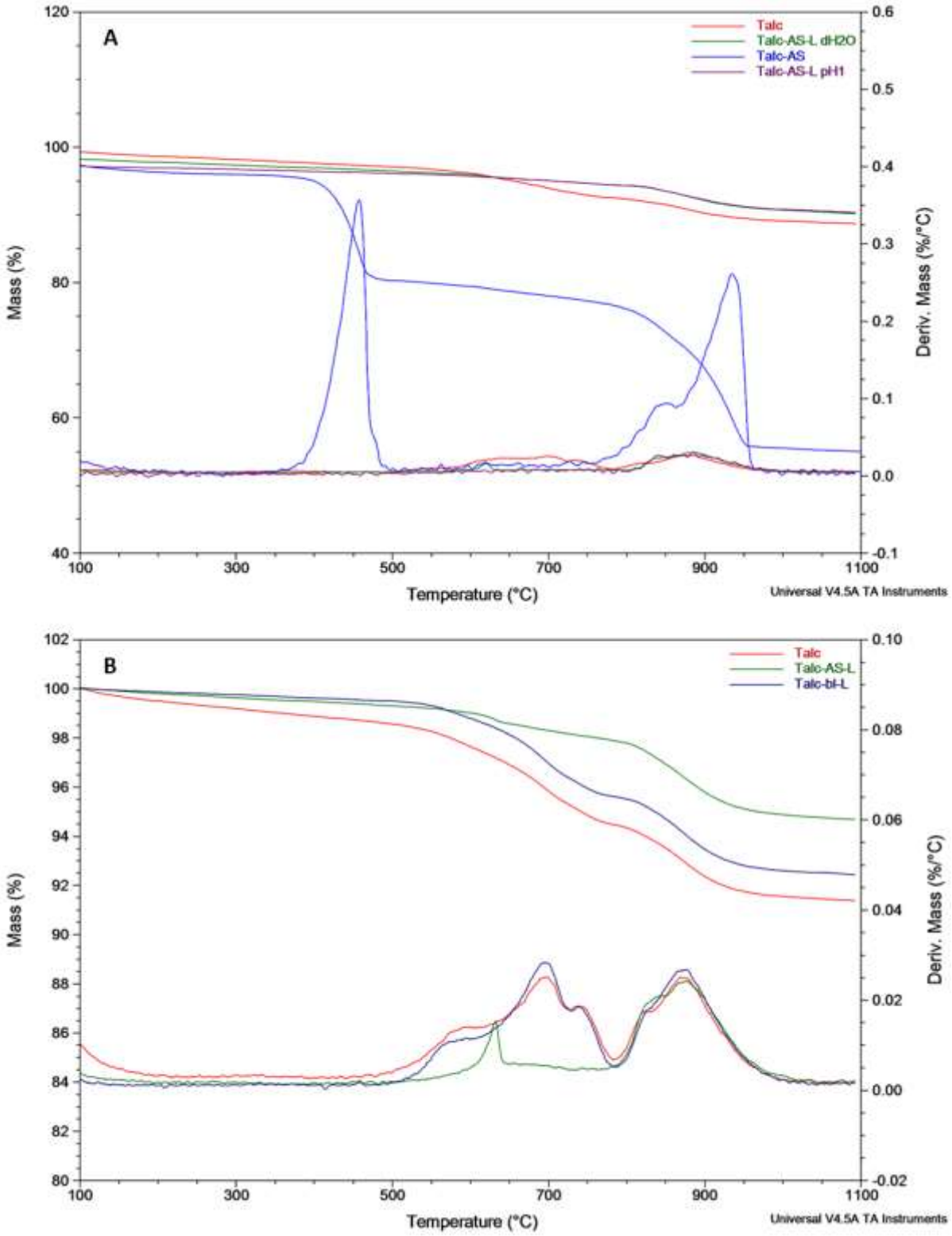

Figure 4 (A) Comparison of TGA of $Talc_{HCl}$ (red) with $Talc_{AS}$ (blue), $Talc_{AS\text{-}L\ H2O}$ (green) and $Talc_{AS\text{-}L\ pH1}$ (purple), and (B) comparison of TGA of $Talc_{HCl}$ (red) with $Talc_{AS\text{-}L\ H2O}$ (green) and $Talc_{H2O}$, (control; navy).

3.2. Reaction of $Talc_{HCl}$ with ammonium sulphate

The thermochemical reaction of $Talc_{HCl}$ with AS generated $Talc_{AS}$ as reaction product. Its mineralogical analysis revealed talc as the main mineral phase. The XRD pattern exhibited the presence of new peaks, which were attributed to metal sulphate ($MgSO_4.6H_2O$) and/or ammonium metal sulphate species (efremovite, $(NH_4)_2Mg_2(SO_4)_3$; boussingaultite, $(NH_4)_2Mg(SO_4)_2.6H_2O$). The lizardite and kaolinite reflections at 2θ values of 12° and 25° were nearly absent from the XRD pattern, which suggested that these phases had reacted with AS to produce the newly-formed sulphate species.

XRD analysis of the leach residue ($Talc_{AS\text{-}L\ pH1}$) obtained from the dissolution of $Talc_{AS}$ in H_2SO_4 at pH = 1.0 (Figure 2) and the one of $Talc_{AS\text{-}L\ H2O}$ obtained from its dissolution in H_2O (result not shown), were identical and featured distinctive reflections at 2θ values of 10°, 19° and 29°. These reflections indicated the composition of talc (> 98%), with traces of lizardite or kaolinite, and the absence of the sulphate species identified in $Talc_{AS}$. These results showed that the parent sample could be further concentrated in talc from 68% in $Talc_{HCl}$ to 98% in $Talc_{AS\text{-}L\ pH1}$ or $Talc_{AS\text{-}L\ H2O}$; this degree of purification could not be achieved with the pre-concentration step in 10% m/m HCl performed on the original talc sample.

TGA analysis of $Talc_{HCl}$, $Talc_{AS}$, $Talc_{AS\text{-}L\ pH1}$ and $Talc_{AS\text{-}L\ H2O}$ (i.e. leach residue from the dissolution of $Talc_{AS}$ in water) was also performed (Figure 4) to complement the XRD results. The mass losses recorded for $Talc_{AS\text{-}L\ pH1}$ and $Talc_{AS\text{-}L\ H2O}$ were identical; they were therefore discussed jointly. The mass loss observed between 400 - 470^{o}C for $Talc_{AS}$ (Figure 4A) was caused by the thermal decomposition of excess, unreacted AS remaining in the sample (Mohammed et al, 2016), whereas those obtained between 800 and 1000^{o}C correspond to dehydroxylation of talc and the loss of SO_3 (Scheidema and Taskinen, 2011) from the decomposition of the metal and ammonium-metal sulphate phases formed from the lizardite and kaolinite during thermochemical treatment with AS.

Figure 4B illustrates the thermal behaviour of $Talc_{HCl}$ *vs* $Talc_{AS\text{-}L\ H2O}$ vs $Talc_{H2O}$. All TGA curves showed an identical mass loss between 850^{o}C and 1000^{o}C, which is the temperature at which talc dehydroxylation occurs. This demonstrated that the amount of talc in $Talc_{HCl}$ and $Talc_{H2O}$ had not been altered by the thermochemical treatment with AS and leaching process, i.e. that talc had not reacted with AS under the thermal condition tested. The finding was further confirmed by the identical DTG curves obtained for these three samples between 850^{o}C and 1000^{o}C. This mass loss of ca. 3.8% indicated a talc content of ca. 80%, which was in agreement with the recorded mass of the leach residues, which represented 80.5% of the original $Talc_{HCl}$ sample mass before reaction with AS. The curves for $Talc_{HCl}$ and $Talc_{H2O}$ also displayed a small mass loss between 550 – 600°C and 600 - 750°C, which is the region in which kaolinite (530 – 590°C) and lizardite (600 - 700^{o}C) are known to dehydroxylate (Földvári, M., 2011).

The FTIR scan of $Talc_{AS}$ had distinct bands between 1050 and 1150 cm^{-1}, which are not present in $Talc_{HCl}$ or the leached $Talc_{AS}$ sample, $Talc_{AS\text{-}L\ H2O}$ (Figure 3). These, as well as the band at 600 cm^{-1}, correspond to the vibrations of the sulphate ion. The band observed at 1409 cm^{-1} was attributed to N - H bond movement (scissoring, bending) from hydrated ammonium metal sulphate species formed during the thermochemical reaction with AS. The sulphate bands were not present in the $Talc_{AS\text{-}L}$ spectrum, which strongly suggested the complete dissolution of sulphate phases to solution.

FESEM images of $Talc_{HCl}$ revealed that the parent sample was made up of individual, irregularly shaped and plate-like particles with varying sizes (Figure 5a). $Talc_{AS}$ exhibited distinctly different features. It consisted of unreacted, irregularly-shaped talc-rich particles similar to those found in $Talc_{HCl}$, which were surrounded by numerous globular structures (Figure 5b). These globular particles were different from the perfectly formed hexagonal structures of metal- and ammonium-metal sulphate species reported previously (Doucet et al., 2016; Mohamed et al., 2016, 2019). They were most likely precursors to similar hexagonal structures, but had nevertheless developed crystalline lattices that could be identified by XRD; longer thermochemical reactions may have induced the growth and conversion of the globular particles into fully-shaped hexagons. $Talc_{AS\text{-}L}$ (Figure 5c-d) consisted of platy

and irregular particles, similar to those observed in $Talc_{HCl}$. No globular morphologies were identified, which indicated their complete dissolution following leaching, as already shown by XRD and TGA.

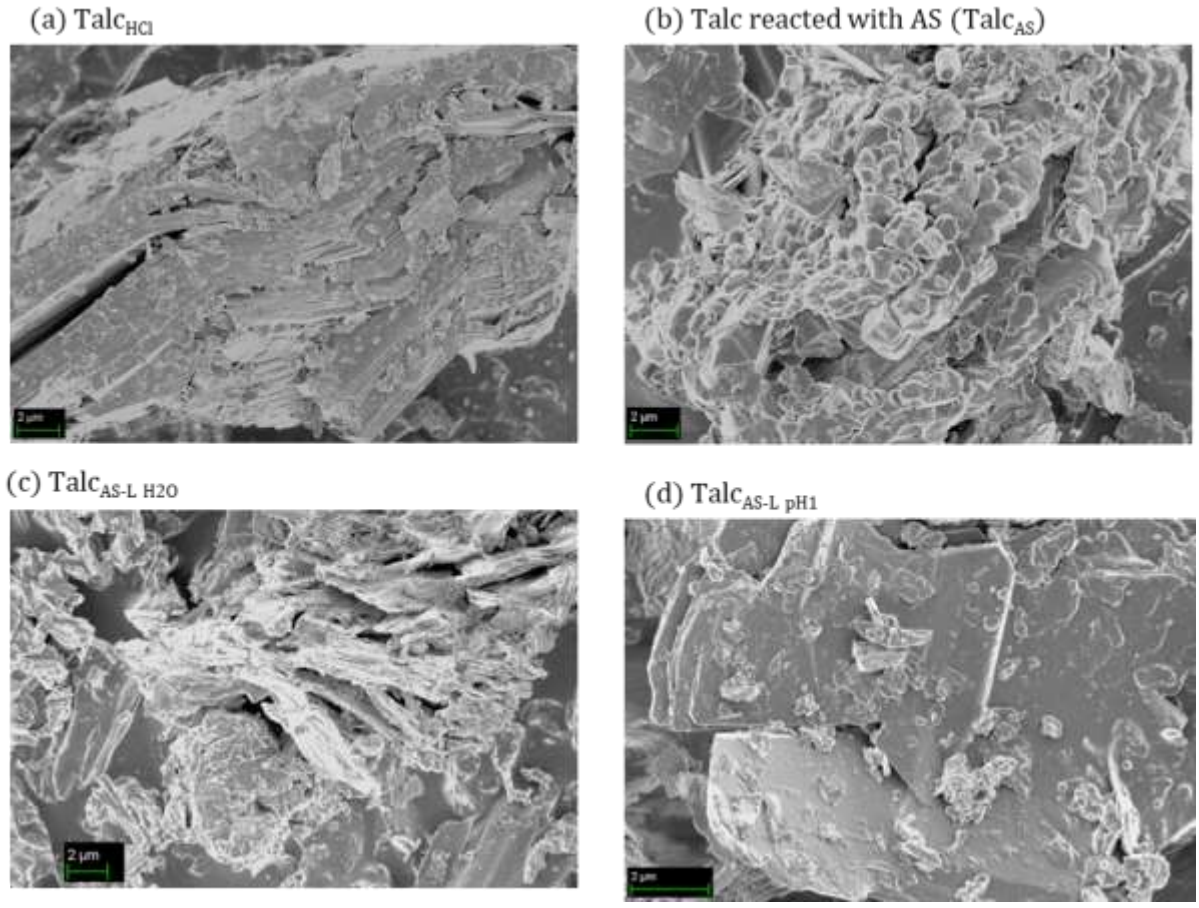

Figure 5 SEM images of $Talc_{HCl}$, $Talc_{AS}$, $Talc_{AS\text{-}L\ H2O}$ and $Talc_{AS\text{-}L\ pH1}$.

4. Conclusions

This study showed that talc exhibits very limited, if any, reactivity with AS when subjected to thermochemical processing under the experimental conditions tested. This thermochemical process of talc with AS may therefore find applications in the field of purification of low-purity talc ore or other talc-bearing materials under the right market conditions, provided the mineral co-exists with phases featuring a high degree of reactivity with AS under thermal conditions. The purified talc obtained in this study is a natural talc, which may have suitable properties for its use, for instance, as a low-cost

alternative in wastewater treatment for the removal of cationic dyes (Grafia et al., 2014). Testing this application was outside the scope of this paper.

Acknowledgements

The authors thank Ms Wiebke Grote for XRD, Ms Jeanette Dykstra for XRF and the University of Pretoria Laboratory for Microscopy and Microanalysis for assistance with FESEM. The authors thank the Council for Geoscience and FJD for providing supervisory assistance, insight and expertise. The project was financially supported by the University of Pretoria and the National Research Foundation of South Africa (NRF Thuthuka Grant No. 117944). Any opinion, finding, conclusion or recommendation expressed in this material is that of the authors and the NRF does not accept any liability in this regard.

References

Ahmed, M.M., Ibrahim, G.A., Hassan, M.M.A., 2007. Improvement of Egyptian talc quality for industrial uses by flotation process and leaching. Int. J. Miner. Process. 83, 132-145.

Alonso, M., Gonzalez, A., De Saja, J.A., 1991. Quality control of mineral impurities in industrial talc by thermogravimetric analysis. Thermochim. Acta. 184, 125-130.

Barani, K., Aghazadeh, V., 2018. Removal of impurities from talc ore by leaching method. J. Chem. Technol. Metall. 53, 296-300.

Bayer, G., Kahr, G. and Mueller-VonMoos, M., 1982. Reactions of ammonium sulphate with kaolinite and other silicate and oxide minerals. Clay Miner. 17, 271-283.

Borra, C.R., Mermans, J., Blanpain, B., Pontikes, Y., Binnemans, K., Van Gerven, T., 2016. Selective recovery of rare earths from bauxite residue by combination of sulfation, roasting and leaching. Miner. Eng. 92, 151-159.

Castillo, L.A., Barbosa, S.E., Maiza, P., Capiati, N.J., 2011. Surface modifications of talcs. Effects of inorganic and organic acid treatments. J. Mater Sci. 46, 2578-2585.

Castillo, L.A., Barbosa, S.E., Maiza, P., Capiati, N.J., 2014. Integrated process for purification of low grade talc ores. Particul. Sci. Technol. 32, 1-7.

De Souza Santos, H., Yada, K., 1988. Thermal transformation of talc as studied by electron-optical methods. Clays Clay Miner. 36, 289-297.

Doucet, F.J., Mohamed, S., Neyt, N., Castleman, B.A. and van der Merwe, E.M., 2016. Thermochemical processing of a South African ultrafine coal fly ash using ammonium sulphate as extracting agent for aluminium extraction. Hydrometallurgy. 166, 174–184.

Dumas, A., Martin, F., Ngo Ke, T., Nguyen, Van H., Nguyen, Viet D., Nguyen, Tat V., Kieu Quy, N., Micoud, P., de Parseval, P., 2015. The crystal chemistry of Vietnamese talcs from the Thanh Son district (Phu Tho province, Vietnam). Clay Miner. 50, 607-617.

Földvári, M., (Ed), 2011. Handbook of Thermogravimetric System of Minerals and Its Use in Geological Practice. Geological Institute of Hungary, Budapest.

Grafia, A.L., Castillo, L.A., Barbosa, S.E., 2014. Use of talc as low-cost clarifier for wastewater. Water Sci. Technol. 69, 640-646.

Hofmeister, A.M., Bowey, J.E., 2006. Quantitative infrared spectra of hydrosilicates and related minerals. Mon. Not. Astron. Soc. 367, 577-591.

Hojamberdiev, M., Arifov, P., Tadjiev, K., Yunhua, X., 2010. Characterization and processing of talc-magnesite from the Zinelbulak deposit. Min. Sci. Technol. 20, 415-420.

Katircioglu-Bayel, D., 2020. Impact of operating parameters on the breakage process of talc. Mining, Metallurgy and Exploration, 37(5), 1717-1727.

Lavikko, S., Eklund, O., 2016a. The significance of the serpentinite characteristics in mineral carbonation by “the ÅA Route”. Int. J. Miner. Process. 152, 7-15.

Lavikko, S., Eklund, O., 2016b. The role of the silicate groups in the extraction of Mg with the ÅA route method. J. CO_2 Util. 16, 466-473.

Li, J., Li, Y., Duan, H., Guo, X., Zhai, Y., 2018. Experimental and kinetic study of magnesium extraction and leaching from laterite nickel ore by roasting with ammonium sulfate. Russ. J. Non-Ferr. Met+ 59, 596-604.

Martin, F., Aymonier, C., Einloft, S, Carême, C., Poirier, M., Claverie, M., Prado, M.A., Dias, G., Quilfen, C., Aubert, G., Micoud, P., Le Roux, C., Salvi, S., Dumas, A., Féry-Forgues, S., 2019. A review of Ni and Co incorporation during talc synthesis: Applications to crystal chemistry, industrial compounds and natural Ni- and Co-rich ore. J. Geochem. Explor. 200, 27-36.

Mohamed, S., van der Merwe, E.M., Altermann, W., Doucet, F.J., 2016. Process development for elemental recovery from PGM tailings by thermochemical treatment: Preliminary major element extraction studies using ammonium sulphate as extracting agent. Waste Manage. 50, 334 – 345.

Mohamed, S., Lehong, K., van der Merwe, E.M., Altermann, W., Doucet, F.J., 2019. Thermochemical treatment of platinum group metal tailings with ammonium salts for major element recovery. J. Therm. Anal. Calorim. 138, 2015–2033.

Nakahira, M., Kato, T., 1963. Thermal transformations of Pyrophyllite and Talc as revealed by X-ray and Electron diffraction studies. Clays Clay Miner. 12, 21-27.

Nduagu, E., Björklöf, T., Fagerlund, J., Wärnå, J., Geerlings, H, Zevenhoven, R., 2012. Production of magnesium hydroxide from magnesium silicate for the purpose of CO_2 mineralisation – Part 1: Application to Finnish serpentinite. Miner. Eng. 30, 75-86.

Orosco, R.P., Ruiz, M.D.C., Barbosa, L.I., González, J.A., 2011. Purification of talcs by chlorination and leaching. Int. J. Miner. Process. 101, 116-120.

Piga, L., Marruzzo, G., 1992. Preconcentration of an Italian talc by magnetic separation and attrition. Int. J. Miner Process 35. 291-297.

Scheidema, M.N., Taskinen, P., 2011. Decomposition Thermodynamics of Magnesium Sulphate. Ind. Eng. Chem. Res. 50, 9550-9556.

Sjöblom, S., Eklund, O., 2014. Suitability of Finnish mine waste (rocks and tailings) for mineral carbonation. Proceedings of ECOS 2014, 27th International Conference on Efficiency, Cost, Optimization, Simulation and Environmental Impact of Energy Systems. Turku, Finland, paper 244.

Soriano, M., Sanchez-Maranon, M., Melgosa, M., Gamiz, E., Delgado, R., 2002. Influence of chemical and mineralogical composition on color for commercial talcs. Color. Res. Appl. 27, 430-440.

Wu, Y., Xu, P., Chen, J., Li, L., Li, M., 2014. Effect of temperature on phase and alumina extraction efficiency of the product from sintering coal fly ash with ammonium sulphate. Chin. J. Chem. Eng. 22, 1363-1367.

Zussman, J., Deer, W., Howie, R.A., (Eds), 2013. Introduction to the Rock-Forming Minerals. Mineralogical Society of Great Britain and Ireland, 3rd edition; pp. 498.